AIP Applied Physics Letters

Ellipticity dependence of 400 nm-driven high harmonic generation

Sabih D. Khan, Yan Cheng, Max Möller, Kun Zhao, Baozhen Zhao et al.

Citation: Appl. Phys. Lett. **99**, 161106 (2011); doi: 10.1063/1.3653277
View online: http://dx.doi.org/10.1063/1.3653277
View Table of Contents: http://apl.aip.org/resource/1/APPLAB/v99/i16
Published by the American Institute of Physics.

APPLIED PHYSICS LETTERS **99**, 161106 (2011)

Ellipticity dependence of 400 nm-driven high harmonic generation

Sabih D. Khan,[1] Yan Cheng,[1] Max Möller,[2,3] Kun Zhao,[2] Baozhen Zhao,[1] Michael Chini,[2] Gerhard. G. Paulus,[3] and Zenghu Chang[2,a)]
[1]*Department of Physics, Kansas State University, Manhattan, Kansas 66506, USA*
[2]*CREOL and Department of Physics, University of Central Florida, Orlando, Florida 32816, USA*
[3]*Institut für Optik und Quantenelektronik, Friedrich-Schiller-Universität Jena, Max-Wien-Platz 1, Jena 07743, Germany*

(Received 9 June 2011; accepted 27 September 2011; published online 18 October 2011)

We studied the dependence of high harmonic generation efficiency on the ellipticity of 400 nm driving laser pulses at 7.7×10^{14} W/cm^2 and compared it with the 800 nm driving laser under the same conditions. The measured decrease of high harmonic yield with the ellipticity of the 400 nm laser is ~1.5 times slower that of the 800 nm, which agrees well with theoretical predictions based on a semi-classical model. The results indicate that it is feasible to use the generalized double optical gating with 400 nm lasers for extracting single attosecond pulses with high efficiency. © *2011 American Institute of Physics*. [doi:10.1063/1.3653277]

Isolated attosecond pulses with a large photon flux are desirable for studying nonlinear processes and for performing attosecond pump-attosecond probe experiments.[1] As the highest on-target pulse energy reported so far is still limited to a few nJ,[2,3] time-resolved attosecond experiments were conducted by combining isolated attosecond pulses with few-cycle femtosecond laser pulses. Isolated attosecond pulses can be produced by sub-cycle gating in high harmonic generation (HHG). Polarization gating (PG),[4,5] double optical gating (DOG)[6,7] and generalized double optical gating (GDOG)[8] are three such methods for generating isolated attosecond pulses, each of them making use of the ellipticity dependence of HHG. They have been demonstrated with 800 nm lasers. It is known that reducing the wavelength of the driving laser is an effective way to increase the photon flux in HHG.[9] Theoretical models predict that the harmonic efficiency scales as λ^{-6} in the plateau region of the HHG spectrum,[10] where λ is the wavelength of driving laser. Experimentally, an energy conversion efficiency of 10^{-4} at ~90 eV HHG photon energy with a 400 nm driving laser has been reported,[11] which is two to three orders of magnitude higher than that from 800 nm lasers. This gives hope to increase the photon flux of isolated attosecond pulses by orders of magnitude.

In this letter, we present measurements of the ellipticity-dependent HHG yield produced by 400 nm driving pulses and compare it with the result for 800 nm driving lasers. Based on the 400 nm ellipticity dependence, we discuss the feasibility of PG, DOG, and GDOG to extract high photon flux isolated attosecond pulses generated by 400 nm driving lasers.

The experimental setup for measuring the ellipticity dependence of HHG with 400 nm lasers is illustrated in Figure 1. The 400 nm driving pulses were produced by frequency-doubling 30 fs, 4.8 mJ, 800 nm pulses from a kHz Ti:sapphire regenerative amplifier using a 300 μm beta barium borate (BBO) crystal (type I phase matching).[12] Two dichroic mirrors that reflect 400 nm and transmit 800 nm light at 45° angle of incidence were utilized to remove the fundamental radiation. The 895 μJ, 400 nm pulses were focused into a 1 mm long helium filled gas cell using a 375 mm focal length silver-coated concave mirror near normal incidence. The HHG spectrum was measured with an XUV grating spectrometer.[7]

The diffraction efficiency of the toroidal grating depends on the angle between the XUV polarization direction and the groove of the grating. To minimize this effect, the ellipticity of the 400 nm light was controlled by a combination of a zero-order half-wave plate and a quarter-wave plate. The optic axis of the latter was fixed while the half-wave plate was rotated to change the ellipticity. As a result, the major axis of the ellipse of the laser light was kept normal to the groove of the grating.[13] Separation of the 400 nm driving laser radiation and the generated harmonics was accomplished by blocking the former using a 300 nm aluminum filter. The ellipticity dependence of the HHG efficiency for the 800 nm laser was obtained using the same experimental setup but with optics designed for 800 nm.

Ellipticity dependences of HHG with 400 nm and 800 nm driving pulses, measured at a peak intensity of 7.7×10^{14} W/cm^2 at the helium gas cell, are presented in Figure 2. The measured harmonic efficiency drops by 90% at ellipticity of 0.31 and 0.21 for 400 nm and 800 nm, respectively. It is clear that the HHG signal is less susceptible to ellipticity for the 400 nm laser.

We developed a theoretical model to explain the effect of the driving laser wavelength on the ellipticity dependence. It is based on the assumption that the dominating contribution to the XUV emission is from the electron trajectories where the transverse displacement in an elliptically polarized field is compensated by an initial transverse velocity when the electron is freed by tunneling.

The laser field is modeled with ellipticity ε and angular frequency ω_0 and assumed as a plane wave that travels in the z direction, $\vec{E}(t)=F/\sqrt{1+\varepsilon^2}[\hat{x}\cos(\omega_0 t)+\hat{y}\varepsilon\sin(\omega_0 t)]$. Here, $\hat{x}$ and $\hat{y}$ are the unit vector in the x and y direction, respectively. Further it is assumed that the electron tunnels out at time t' close to the maximum of the field and with zero initial velocity in the x direction, i.e., along the major axis of the ionizing field. Coulomb effects to the trajectory are

a)Author to whom correspondence should be addressed. Electronic mail: Zenghu.Chang@ucf.edu.

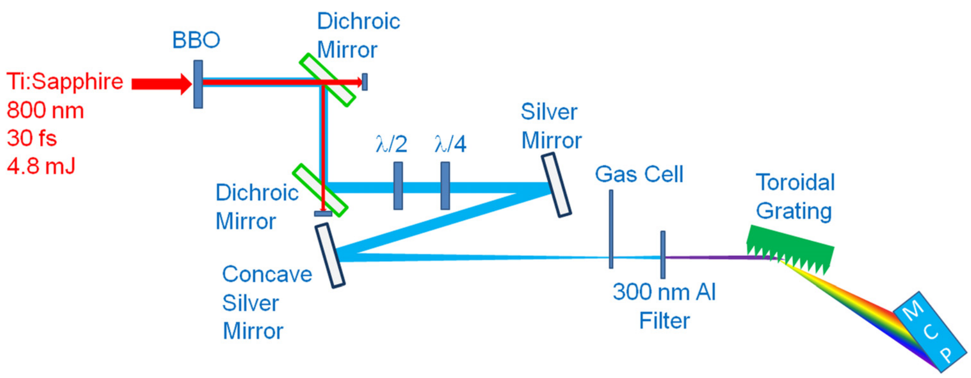

FIG. 1. (Color online) Setup for measuring the ellipticity dependence of HHG with 400 nm laser.

ignored and atomic units are used. Integrating Newton's equations yields the electron's displacement along the y-axis,

$$y=\frac{\varepsilon}{\sqrt{1+\varepsilon^2}}\frac{F}{\omega_0^2}[\sin(\omega_0 t)-\sin(\omega_0 t')-\cos(\omega_0 t')\omega_0(t-t')] \\ +v_{\perp 0}(t-t'), \tag{1}$$

where $v_{\perp 0}$ is an initial perpendicular velocity along the y-axis.

The XUV emission is maximized if the electron returns to the ion, i.e., the origin, at a later collision time $t > t'$. In the strong field regime, effects due the magnetic component can be ignored and thus $z = 0$ is fulfilled. However, the electron can never return to $x(t) = y(t) = 0$ if it is released with zero perpendicular velocity $v_{\perp 0} = 0$, whereas a nonzero perpendicular velocity $v_{\perp 0} \neq 0$ allows such a return. Thus, an efficient recombination occurs when the perpendicular displacement is compensated by the initial perpendicular velocity, i.e., when $y(t) = 0$ in Eq. (1) is reached at time at t,

$$v_{\perp 0} = \frac{\varepsilon}{\sqrt{1+\varepsilon^2}}\frac{F}{\omega_0}\left[\cos(\omega_0 t') - \frac{\sin(\omega_0 t)-\sin(\omega_0 t')}{\omega_0 t - \omega_0 t'}\right]. \tag{2}$$

In the case of small ellipticity ($\varepsilon \ll 1$), one can approximate $x(t) = 0$ with the results for linear polarization where the tunneling phase $\omega_0 t' = 0.107 \times 2\pi$ and the return phase $\omega_0 t = 0.55 \times 2\pi$ are found to generate mid-plateau harmonics from the short trajectories.[13] This results in $v_{\perp 0} = 1.12\varepsilon F/\omega_0$ using Eq. (2). Apparently, the required perpendicular velocity is higher for larger ellipticity.

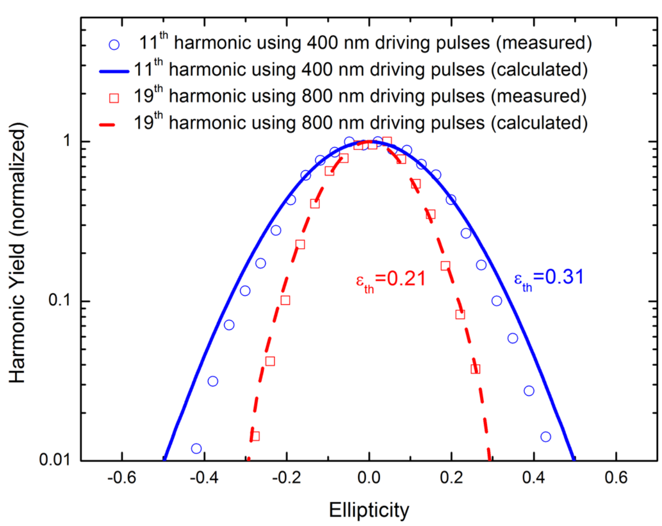

FIG. 2. (Color online) Normalized harmonic yield as a function of ellipticity in helium for the 19th harmonic using 800 nm driving laser (squares) and the 11th harmonic using 400 nm driving laser (circle). Peak intensity for both cases was 7.7×10^{14} W/cm^2. The results from semi-classical calculations using the experimental parameters are shown for comparison (solid and dashed lines for 400 nm and 800 nm, respectively).

The probability for the electron to tunnel out with a perpendicular velocity has been discussed theoretically[14] and tested experimentally.[15] Using the results from above, one finds

$$\frac{I_{XUV}(\varepsilon)}{I_{XUV}(\varepsilon=0)} \approx \frac{w(v_{\perp 0})}{w(v_{\perp 0}=0)} = e^{-\frac{\sqrt{2I_p}v_{\perp 0}^2}{F/\sqrt{1+\varepsilon^2}}} \approx e^{-\frac{\sqrt{2I_p}v_{\perp 0}^2}{F}} \\ = e^{-\frac{1.25\sqrt{2I_p}F}{\omega_0^2}\varepsilon^2}. \tag{3}$$

Here, I_p is the ionization potential of the target atom.

In this picture, the HHG yield at increased ellipticity is lower due to the fact that electrons with larger perpendicular velocity have a smaller tunneling rate. This analytical result indicates that the ellipticity dependence of the high harmonic field is nearly Gaussian, with increasing width for lasers with higher carrier frequency. This is consistent with our comparison of the HHG signal from 800 nm and 400 nm lasers at the same field strength and ellipticity. Target atoms with higher ionization potential and higher field strengths are expected to result in narrower ellipticity dependence.

Equation (3) is valid for ellipticity $\varepsilon \ll 1$. For an arbitrary ellipticity, the electron releasing and return time need to be obtained by solving the electron's equation of motion in the x and y directions numerically. The numerically calculated ellipticity dependence is included in Figure 2. The calculated results agree quite well with the experiments.

The weaker dependence of HHG on ellipticity at 400 nm as compared to 800 nm affects the design of gating schemes for isolated attosecond pulse generation. When the driving laser in PG, DOG, and GDOG is created by superimposing two counter-rotating elliptically polarized fields, the width of the gate where the driving laser is linearly polarized can be expressed as,

$$\delta t = \frac{\alpha}{\ln(2)}\varepsilon_{th}\frac{\tau_p^2}{T_d}, \tag{4}$$

where α is 1 for PG and DOG and 0.5 for GDOG,[8,13] τ_p is the pulse duration of the driving pulse, and T_d is the delay between the two counter-rotating elliptically polarized fields. The threshold ellipticity, ε_{th}, defined as the ellipticity at which the harmonic yield has dropped by an order of magnitude, is 0.31 for 400 nm driving pulses and 0.21 for 800 nm driving pulses, see Figure 2. Larger ε_{th} requires larger delay to achieve the same polarization gate. This results in a lengthened leading edge of the pulse and therefore increases the ground state depletion at the time of the gate.

We calculated the required delay T_d for 400 nm laser pulses as a function of pulse width and estimated the ground state depletion using the Ammosov-Delone-Krainov (ADK) rate[16] in supplementary material.[17] We found that a 400 nm pulse comprised of about five optical cycles ($\tau_p = 6.5$ fs) can produce single attosecond pulse using GDOG without completely depleting the ground state. The delay required for GDOG is 6.9 fs, which is comparable to the laser pulse duration of 6.5 fs. This is desirable to maintain high laser intensity inside the gate. Sub-10 fs 400 nm pulses have been generated by pulse compression through self-phase modulation in gas-filled hollow core fiber.[18–20]

In conclusion, our measurements show that the HHG yield from a 400 nm driving laser drops more slowly with increasing ellipticity than that of 800 nm driving lasers. We expect that the generalized double optical gating is appropriate to take advantage of the increased conversion efficiency at short driving laser wavelengths in generating high energy isolated attosecond pulses. This material is supported by the U.S. Army Research Office, and by U.S. Department of Energy and by National Science Foundation.

1. Z. Chang and P. Corkum, J. Opt. Soc. Am. B **27**, 9 (2010).
2. H. Mashiko, S. Gilbertson, C. Li, E. Moon, and Z. Chang, Phys. Rev. A **77**, 063423 (2008).
3. F. Ferrari, F. Calegari, M. Lucchini, C. Vozzi, S. Stagira, G. Sansone, and M. Nisoli, Nat. Photonics **4**, 875 (2010).
4. P. B. Corkum, N. H. Burnett, and M. Y. Ivanov, Opt. Lett. **19**, 1870 (1994).
5. Z. Chang, Phys. Rev. A **70**, 043802 (2004).
6. Z. Chang, Phys. Rev. A **76**, 051403(R) (2007).
7. H. Mashiko, S. Gilbertson, C. Li, S. D. Khan, M. M. Shakya, E. Moon, and Z. Chang, Phys. Rev. Lett. **100**, 103906 (2008).
8. X. Feng, S. Gilbertson, H. Mashiko, H. Wang, S. D. Khan, M. Chini, Y. Wu, K. Zhao, and Z. Chang, Phys. Rev. Lett. **103**, 183901 (2009).
9. B. Shan and Z. Chang, Phys. Rev. A **65**, 011804(R) (2001).
10. E. L. Falcão-Filho, V. M. Gkortsas, A. Gordon, and F. X. Kärtner, Opt. Express **17**, 11217 (2009).
11. E. L. Falcão-Filho, C. Lai, K. Hong, V. M. Gkortsas, S. Huang, L. Chen, and F. X. Kärtner, Appl. Phys. Lett. **97**, 061107 (2007).
12. C. Yun, S. Chen, H. Wang, M. Chini, and Z. Chang, Appl. Opt. **48**, 5127 (2009).
13. Z. Chang, *Fundamentals of Attosecond Optics*, 1st ed. (CRC, Boca Raton, 2011), p. 251, ISBN-10:1420089374.
14. M. Y. Ivanov, M. Spanner, and O. Smirnova, J. Mod. Opt. **52**, 165 (2005).
15. L. Arissian, C. Smeenk, F. Turner, C. Trallero, A. V. Sokolov, D. M. Villeneuve, A. Staudte, and P. B. Corkum, Phys. Rev. Lett. **105**, 133002 (2010).
16. Z. Chang, *Fundamentals of Attosecond Optics*, 1st ed. (CRC, 2011), p. 184, ISBN-10: 1420089374.
17. See supplementary material at http://dx.doi.org/10.1063/1.3653277 for comparison of delay T_d and ground state depletion as a function of pulse duration τ_p.
18. J. Liu, K. Okamura, Y. Kida, T. Teramoto, and T. Kobayashi, Opt. Express **18**, 20645 (2010).
19. J. Liu, Y. Kida, T. Teramoto, and T. Kobayashi, Opt. Exp. **18**, 4664 (2010).
20. O. Duhr, E. T. J. Nibbering, G. Korn, G. Tempea, and F. Krausz, Opt. Lett. **24**, 34 (1999).